Computer Engineering and Applications Vol. 7, No. 3, October 2018

A Vector Potential Function-Based Collision Avoidance Control for Differential-Steered Robots

Anugrah K. Pamosoaji

Faculty of Industrial Technology, Universitas Atma Jaya Yogyakarta, Indonesia
School of Mechanical Engineering, Pusan National University, Busan, South Korea
anugrah.pamosoaji@uajy.ac.id

ABSTRACT

A collision avoidance control that tracks a vector potential field-based velocity plan of a differential-steered robot is designed. Vector potential function (VPF) is a type of potential function used for motion planning. The plan resulted by the VPF is the desired velocity vector of the robot on all points in collision-free space. The problem to address in this paper is velocity tracking control in the environment of a circular obstacle. A controller is designed to track the VPF-based velocity plan. A concept of collision cone will be used to evaluate the ability of the controller to avoid collision between the robot and the obstacle. The stability of the controller is verified by using the Lyapunov stability analysis. Simulations of the controller's performance are presented.

Keywords: Motion Planning, Vector Potential Field, Velocity Tracking, Collision Avoidance

1. INTRODUCTION

Collision avoidance is a mature issue in robotics research. Particularly, almost all research in path and trajectory planning and control involve such the issue. Early years of robotics path and trajectory planning research was marked by some fundamental results on artificial potential function introduced in [1-2]. The last publication became a cornerstone for myriads of results in path planning studies. The main principle is straightforward: a collision-free space can be modeled as a potential function such that the lowest value of the function will be located at the target point. Meanwhile, the points on the space occupied by some obstacles will have very high values. Therefore, if a robot is initially located at a collision-free point, it will be driven to the target automatically. Some variants on this method were introduced, such as the research reported in [3-6].

Instead of regarding collision avoidance as global planning problem, some studies treated this issue as local planning problem. For instance, the work reported in [7]. Here, a technique of vector field histogram (VFH) became one of the best methods in collision avoidance studies. The VFH method is based on the segmentation of the overall space, such that the edges of the obstacles can be detected by evaluating the value of each cell. Other publications were proposed to anticipate incidental presence of some obstacles. The proposed methods were dynamic window approach [8], and nearness diagram [9].

As the research in collision avoidance become mature in the latest decades, questions of safety appeared. The addressed issue is described as follows. Suppose

that the position and orientation of a robot is in a collision-free space. How can we guarantee that the robot is in a safe position? [10]. Such the problem appears by considering that in reality, the obstacles may be dynamic. Even though the position of the robot is on the collision-free space, however its linear velocity and the obstacles' linear velocities may cause a collision in the near future. The work in [11] successfully performed a concept of collision cone to describe the possibility of collision. This concept was further developed into the concept of reciprocal velocities [12-14].

One problem found in reciprocal velocities concept is that there is no specific method to determine the maximum allowable linear velocity to lead the robot staying outside its velocity obstacle [12], [15-16]. To solve the problem, an integration of planning and control phase is proposed. The planning phase is based on real-time velocity plan called "vector potential function-based motion plan" is proposed in this paper. This method was introduced in [17]. The main principle is that a velocity vector field will be generated in the environment of a circular obstacle by a vector potential function defined at the obstacle's center. The generated velocity vector field must be tracked by the robot. Therefore, a velocity tracking control law is proposed in this paper. A parameter setting is proposed such that the resulted velocity satisfies the constraint in the velocity obstacle of the robot.

The organization of the paper is described as follows. Section 2 presents the problem description, starting from the kinematics and dynamics model of differential-steered mobile robots and the introduction to collision cone, and finally, the objective of this study. Section 3 explains the designed velocity tracking control law based on vector potential function (VPF). Section 4 describes the simulation results revealing the performance of the proposed control law. Finally, section 5 provides the conclusion of this study.

2. PROBLEM DESCRIPTION

2.1 KINEMATICS AND DYNAMICS MODEL OF DIFFERENTIAL-STEERED MOBILE ROBOT

Consider a mobile robot, each with a simplified kinematics model adopted from [18] given as,

$$\begin{aligned} \dot{x} &= v\cos\theta, \\ \dot{y} &= v\sin\theta, \\ \dot{\theta} &= \omega, \end{aligned} \tag{1}$$

where (x, y, θ), v and ω represent the configuration (position and orientation) of the robot, the nominal linear velocity and the nominal angular velocity of the robot, respectively; Let O be the center of gravity of the *i*-th robot; C be the passive wheel assembled at the rear of the robot; b be the distance between C and O; d be the distance between the right and left wheels.

The dynamics of the robot is investigated by using Newtonian dynamics. Let us define F_{lx} and F_{rx} as the left and right longitudinal tire forces resulted from the

ISSN: 2252-4274 (Print)
ISSN: 2252-5459 (Online)

wheels' motion, respectively; F_{ly} and F_{ry} represent the left and right lateral tire forces on the left and right wheels, respectively; f_x and f_y are the longitudinal and lateral forces on the castor wheel, respectively. Let m be the mass of the robot. We define ω_l and ω_r as the nominal angular velocities of the left and right wheels, respectively.

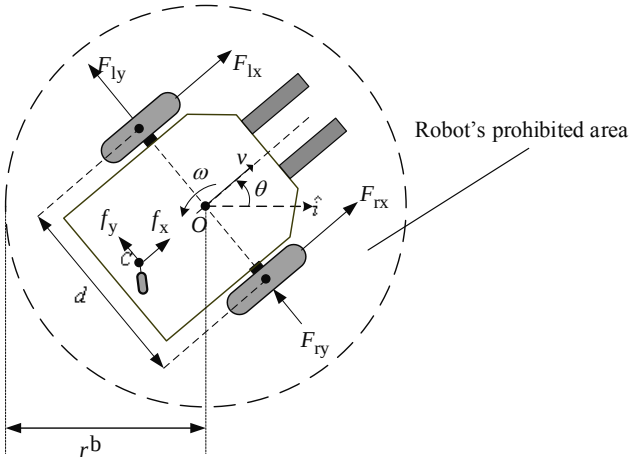

FIGURE 1. Kinematics and Dynamics Model of Differential-Steered Mobile Robot.

The relations between ω_l, ω_r, v, and ω are described in the following equations below [18],

$$v = \frac{1}{2}(r(\omega_r + \omega_l)) \tag{2}$$

$$\omega = \frac{1}{d}(r(\omega_r - \omega_l)) \tag{3}$$

By using Newton's laws, the equation of motions of the robot can be derived as follows. The forces applied on the longitudinal, lateral, and the moment applied on the center of gravity O are described as follows;

$$m\dot{v}^a = F_{lx} + F_{rx} + f_x, \tag{4}$$

$$mv^a\omega_i^a = F_{ly} + F_{ry} + f_y, \tag{5}$$

$$I_z\dot{\omega}^a = \frac{d}{2}(F_{rx} - F_{lx}) - bf_y, \tag{6}$$

where v^{a} and ω^{a} are the actual values of v and ω, respectively.

The actuators are two identical DC motors installed on the left and right wheels, where each wheel is represented by the following parameters [18]: k_a and k_b the torque constant and voltage constant multiplied by the gear ratio; R_a is the electric resistance constant. The right and the left motors produce torques τ_r and τ_l, respectively, that are formulated as,

$$\tau_r = k_a\left(v_r - k_b\omega_r^a\right)/R_a\,, \tag{7}$$

$$\tau_l = k_a\left(v_l - k_b\omega_l^a\right)/R_a\,, \tag{8}$$

where v_r and v_l are the input voltages to the right and left motor, respectively. The dynamic equations of both of the motors and wheels are expressed as,

$$I_w\dot{\omega}_{i,r}^a + B_w\omega_r^a = \tau_r - rF_{rx}\,, \tag{9}$$

$$I_w\dot{\omega}_l^a + B_w\omega_l^a = \tau_l - rF_{lx}\,, \tag{10}$$

where I_w and B_w are defined as the moment of inertia and the viscous friction coefficient of motor's rotor-gearbox-wheel combination, respectively.

Define k_p and k_D as the proportional and derivative constants for a PD controller of the motor, respectively; the equation of motion of the robot can be formulated as the simplification of the model presented in [18] as

$$\mathbf{A}\begin{bmatrix}\dot{\omega}_r^a\\ \dot{\omega}_l^a\end{bmatrix} + \mathbf{B}\begin{bmatrix}\omega_r^a\\ \omega_l^a\end{bmatrix} + \mathbf{f} = \mathbf{C}\begin{bmatrix}\omega_r\\ \omega_l\end{bmatrix}, \tag{11}$$

where

$$\mathbf{A} = \begin{bmatrix} I_w + \dfrac{k_a k_D r}{R_a} + \dfrac{r^2 m_i}{4} + \dfrac{r^2 I_{i,z}}{d^2} & -\left(\dfrac{r^2 I_{i,z}}{d^2} - \dfrac{r^2 m_i}{4}\right) \\ -\left(\dfrac{r^2 I_{i,z}}{d^2} - \dfrac{r^2 m_i}{4}\right) & I_w + \dfrac{k_a k_D r}{R_a} + \dfrac{r^2 m_i}{4} + \dfrac{r^2 I_{i,z}}{d^2} \end{bmatrix}, \tag{12}$$

$$\mathbf{B} = \begin{bmatrix} B_w + \dfrac{k_a k_b}{R_a} + \dfrac{k_a k_P r}{R_a} & 0 \\ 0 & B_w + \dfrac{k_a k_b}{R_a} + \dfrac{k_a k_P r}{R_a} \end{bmatrix}, \tag{13}$$

ISSN: 2252-4274 (Print)
ISSN: 2252-5459 (Online)

$$\mathbf{f} = \begin{bmatrix} -\frac{r}{2} f_{\mathrm{x}} + \frac{rb}{d} f_{\mathrm{y}} \\ -\frac{r}{2} f_{\mathrm{x}} + \frac{rb}{d} f_{\mathrm{y}} \end{bmatrix}, \tag{14}$$

$$\mathbf{C} = \begin{bmatrix} \frac{k_{\mathrm{a}} k_{\mathrm{p}} r}{R_{\mathrm{a}}} & 0 \\ 0 & \frac{k_{\mathrm{a}} k_{\mathrm{p}} r}{R_{\mathrm{a}}} \end{bmatrix}, \tag{15}$$

2.2 COLLISION CONE

The term "collision cone" was introduced in Chakravarthy and Ghose (1998). A collision cone is a collection of points such that the robot will eventually collide to the obstacle. The principle of collision cone is motivated by a fact that to analyze the possibility of collision, we could not evaluate only the configuration (position and orientation) of the robot. As shown in Fraichard and Asama (2004), the linear velocity of the robot must be considered as well.

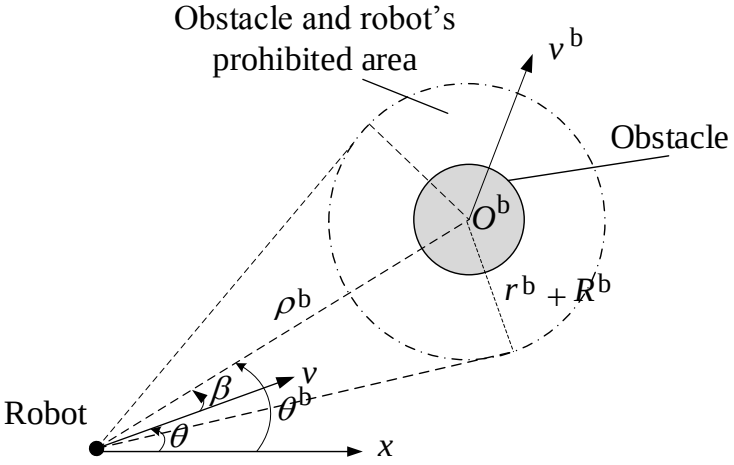

FIGURE 2. Collision cone.

In this paper, the control system would be designed such that the robot could perform collision avoidance motions based on Lemma 2 introduced in Chakravarthy and Ghose (1998). To discuss this paradigm, the readers are suggested to see Figure 2. Define ρ^{b} as the distance between the center of mass of the robot and the center of the vehicle; θ^{b} as the inclination angle of the vehicle-to-obstacle line with respect to global *x*-axis.

According to the Lemma 2 in Chakravarthy and Ghose (1998), a robot must be in collision in the future if and only if the conditions of $\rho^{\mathrm{b}}\dot{\theta}^{\mathrm{b}} = 0$ and $\dot{\rho}^{\mathrm{b}} < 0$ are satisfied. It can be inferred from the lemma that the collision might be avoided if and only if $\rho^{\mathrm{b}}\dot{\theta}^{\mathrm{b}} \neq 0$ or $\dot{\rho}^{\mathrm{b}} \geq 0$. Therefore, it is straightforward that the second

condition would guarantee the successfulness of avoiding collision motions. However, since the first condition might be occurred for all values of $\dot{\rho}^{\mathrm{b}}$, then it must be evaluated further.

Define r^{b} and R^{b} as the robot's and obstacle's radius of prohibited area, respectively. As shown in Figure 2, we model a robot as its center of mass and the obstacle as a circle with radius $r^{\mathrm{b}} + R^{\mathrm{b}}$. It is clear that if $|\beta| < \arcsin\left(\frac{r^{\mathrm{b}} + R^{\mathrm{b}}}{\rho^{\mathrm{b}}}\right)$ and $\dot{\rho}^{\mathrm{b}} < 0$ then there exist a finite time *t* where a collision occurs, i.e, the robot enters the prohibited area of the obstacle.

2.3 OBJECTIVE OF THE RESEARCH

The objective of the research can be described as follows. Consider a wheeled mobile robot whose kinematics and dynamics model are described in Equation (1) and Equations (11) - (15), respectively. Moreover, consider a scenario of the robot facing an obstacle while moving towards a specified target, as shown in Figure 2. Design a control law such that the robot can perform a collision avoidance motion against the circular obstacle.

3. COLLISION AVOIDANCE CONTROL LAW DESIGN

In this study, the integration of planning and control is applied. First of all, a velocity planning algorithm to avoid collision from Pamosoaji and Hong (2013) is used. The planning algorithm uses vector potential function (VPF) and generates linear velocity vectors for all points in the environment of the obstacle. The performed plan then is tracked by applying a velocity tracking control law (see sub-section 3.2).

3.1 VECTOR POTENTIAL FUNCTION (VPF)

Vector potential function (VPF) is function used to generate velocity plan in a free-collision space. This function is inspired from the Basic Physics course, i.e., Biot-Savart law on electric current flowing through a cable with infinite length (Pamosoaji and Hong, 2013). For the context of collision avoidance over a circular obstacle, velocity plan can be generated by applying curl operator to the following function,

$$\boldsymbol{\psi} = \kappa_{\psi} \int_{-L}^{L} \left(\rho^2 + z^2\right)^{-1/2} dz\, \mathbf{k}, \qquad (16)$$

where ψ is the VPF applied on the center of the obstacle, κ_{ψ} is a positive constant; ρ is the distance between the center of robot, i.e., *O*, and the center of the obstacle, and z denotes the length of the "cable" passing through the obstacle orthogonally. Therefore, the generated velocity plan, denoted as U is formulated as,

ISSN: 2252-4274 (Print)
ISSN: 2252-5459 (Online)

$$\mathbf{U} = \nabla \times \boldsymbol{\psi} = \frac{\kappa_{\psi}}{\rho}\left(\sin\left(\beta+\theta\right)\mathbf{i} - \cos\left(\beta+\theta\right)\mathbf{j}\right) \tag{17}$$

As shown in Pamosoaji and Hong (2013), the resulted $\mathbf{U}$ is a velocity vector field with tangent direction to the line connecting the occupied point to the center of the obstacle.

3.2 CONTROL LAW DESIGN

In this paper, a control law is designed such that the error $\tilde{v}$ between the resulted plan in Equation (17), i.e.,

$$\tilde{v} = v - \left\|\mathbf{U}\right\|, \tag{18}$$

equals to zero. From Equation (17) it can be concluded that $\left\|\mathbf{U}\right\| = \frac{\kappa_{\psi}}{\rho_k^{\mathrm{b}}}$. Consider the following kinematic model,

$$\dot{\tilde{v}} = \dot{v}, \tag{19}$$

$$\dot{\beta}^{\mathrm{b}} = -\omega + \frac{v}{\rho^{\mathrm{b}}}\sin\beta^{\mathrm{b}}. \tag{20}$$

Proposition 1: The following control law:

$$\dot{v} = -\left(\frac{\chi - 1}{\rho^{\mathrm{b}}}\right)\left(R^{\mathrm{b}} + r^{\mathrm{b}}\right)\kappa^{\mathrm{b}}, \tag{21}$$

$$\omega = k_{\omega}\left(\beta^{\mathrm{b}} - \pi/2\right) + v/\rho^{\mathrm{b}}\sin\beta^{\mathrm{b}}, \tag{22}$$

where

$$\chi = \tanh\left(\mathrm{sign}\left(\frac{v}{\rho^{\mathrm{b}}} - \frac{\kappa_k^{\mathrm{b}}}{\left(\rho^{\mathrm{b}}\right)^2}\right)k_{\chi}\cos\beta^{\mathrm{b}}\right) + 1 \tag{23}$$

makes the origin of Equation (19)-(20) globally asymptotically stable if and only if $\cos\beta^{b} \geq 0$.

Proof: Define a Lyapunov candidate function

$$V^{b} = 1/2\left(\beta^{b} - \pi/2\right)^{2} + 1/2\left(v - \kappa^{b}/\rho^{b}\right)^{2} \quad (24)$$

The time derivative of V_{k}^{b} can be expressed as,

$$\dot{V}^{b} = \left(\beta^{b} - \pi/2\right)\left(v/\rho^{b}\sin\beta^{b} - \omega\right) + \left(v - \kappa^{b}/\rho^{b}\right)\dot{v}. \quad (25)$$

Applying the control law in Equations (21) - (22) to (25) yields the following expression for $\dot{V}_{k}^{b}$;

$$\dot{V}^{b} = -\left(\beta^{b} - \pi/2\right)^{2} - \left(\frac{v}{\rho^{b}} - \frac{\kappa^{b}}{\left(\rho^{b}\right)^{2}}\right)(\chi - 1)\left(R^{b} + r^{b}\right)\kappa^{b}. \quad (26)$$

Substitution of χ in Equation (23) to (26) yields,

$$\dot{V}^{b} = -\left(\beta^{b} - \pi/2\right)^{2} - \left|\frac{v}{\rho^{b}} - \frac{\kappa^{b}}{\left(\rho^{b}\right)^{2}}\right|\left(R^{b} + r^{b}\right)\kappa^{b}\tanh\left(k_{\chi}\cos\beta^{b}\right). \quad (27)$$

Therefore, the origin of Equation (19) - (20) is asymptotically stable if and only if. To anticipate the robot to enter an intersection area of more than one obstacle, the velocity plan then is generated by using the VPF from the closest obstacle.

4. SIMULATION RESULTS

A simulation was performed to evaluate the performance of the proposed collision avoidance control design. Here, three mobile robots were involved. The configurations of robots I, II, and III were $(20\text{m}, -10\text{m}, \pi\,\text{rad})$, $(20\text{m}, 10\text{m}, -\pi/6\,\text{rad})$, and $(0\text{m}, 20\text{m}, \pi/2\,\text{rad})$, respectively.

ISSN: 2252-4274 (Print)
ISSN: 2252-5459 (Online)

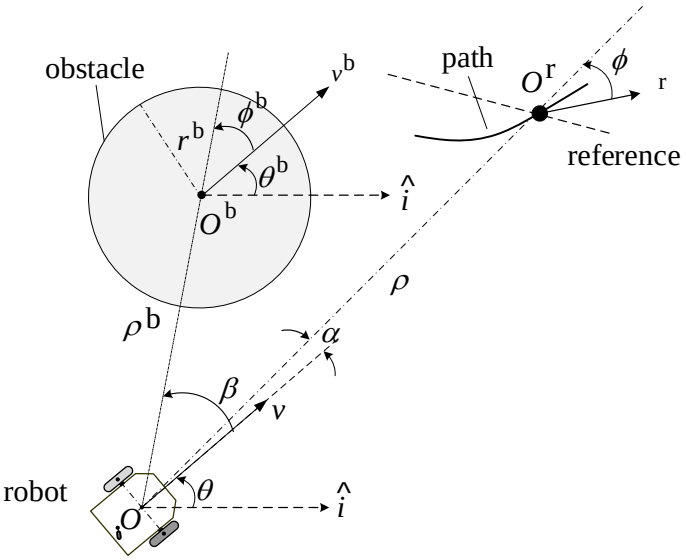

FIGURE 3. Target tracking with the existence of a circular obstacle.

The scenario is described as follows. Each robot was assigned to follow an associated moving reference. The configurations of the references of robots I, II, and III were $(20\text{m}, 40\text{m}, 0\,\text{rad})$, $(-20\text{m}, -40\text{m}, 0\,\text{rad})$, and $(60\text{m}, -40\text{m}, \pi/2\,\text{rad})$, respectively. The scenario was designed such that the references only moved forward with linear velocities set to 1 m/s and without any turning maneuver. Here, the length of $r_k^{\text{b}} + R_k^{\text{b}}$ was set as 10 meters. The controller's constant was set as $k_\chi = 100$, $k_\omega = 5\,\text{sec}^{-1}$. The dynamics parameters of the robots are described in Table 1. Here, the actuators were assumed to be controlled by using a PD-controller. The scenario of the mission is illustrated in Figure 3.

For target tracking mission, a set of navigation variables was used, i.e., ρ, ϕ, and α, where the definitions are explained in Equation (28):

$$\begin{bmatrix} \rho \\ \phi \\ \alpha \end{bmatrix} = \begin{bmatrix} \sqrt{\Delta x^2 + \Delta y^2} \\ \arctan 2(\Delta y, \Delta x) - \theta_{\text{g}} \\ \arctan 2(\Delta y_i, \Delta x_i) - \theta_i \end{bmatrix}, \tag{28}$$

$$\Delta x = x^{\text{r}} - x, \tag{29}$$

$$\Delta y = y^{\text{r}} - y. \tag{30}$$

The tracking control law used is expressed as follows,

$$v = k_v \rho \cos\alpha, \tag{31}$$

$$\omega = \tanh(\rho)\left(k_\omega \alpha - \frac{v^r}{\rho}\sin\phi + \frac{v}{\rho}\sin\alpha \right), \qquad (32)$$

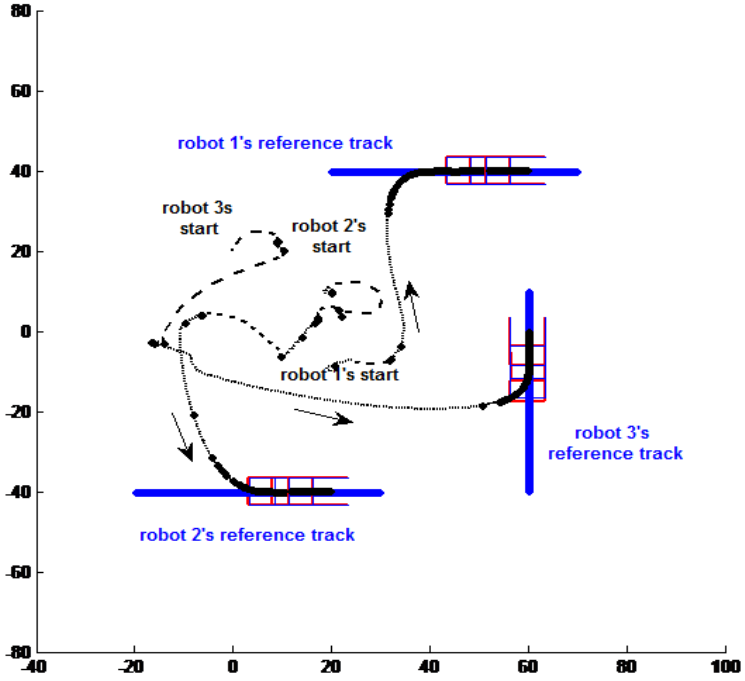

FIGURE 4. Trajectories performed by 3 vehicles to avoid inter-robot collision.

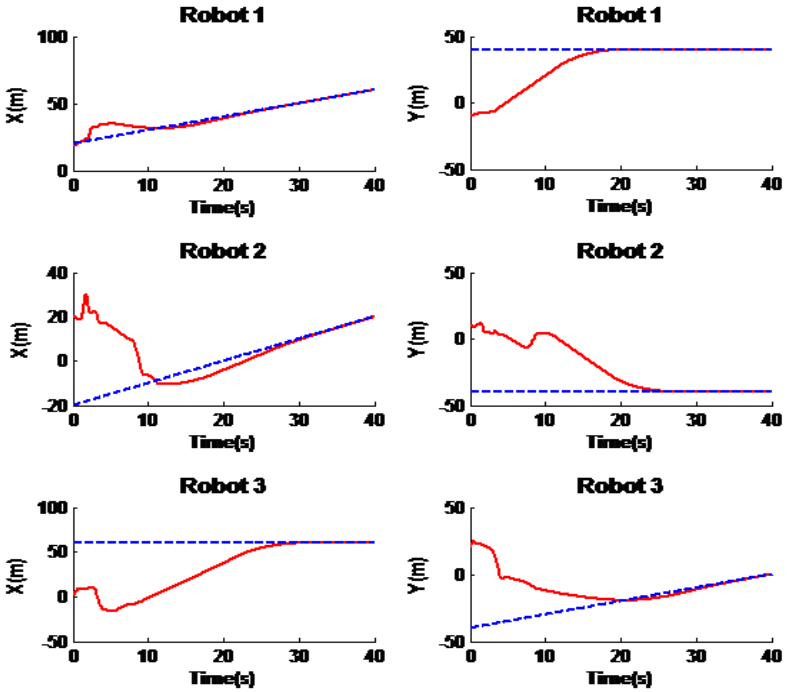

FIGURE 5. Reference tracking results of the three robots. The red-and-solid curves represent the actual values of the robot's coordinate and the blue-and-dotted curves represent the reference of the associated robots.

ISSN: 2252-4274 (Print)
ISSN: 2252-5459 (Online)

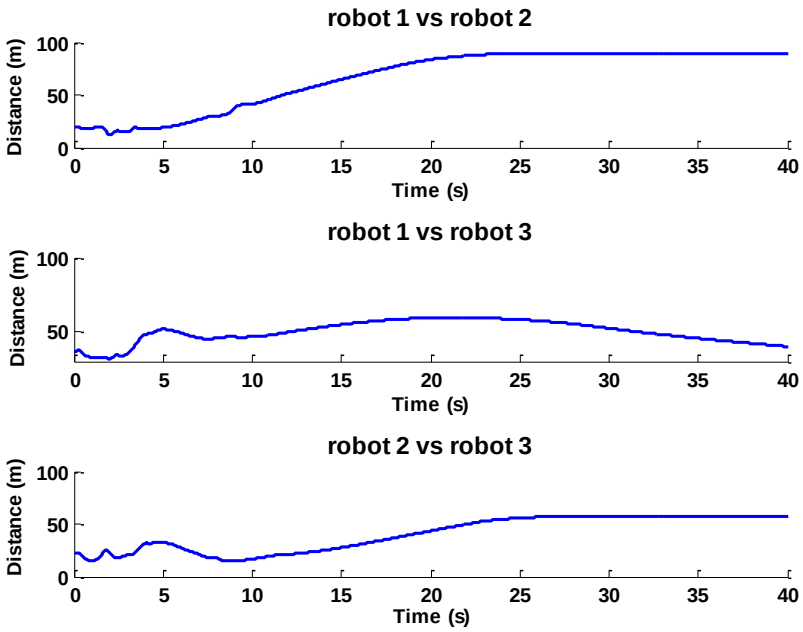

FIGURE 6. The distance between any pair of robots.

TABLE 1.
Dynamics parameters used in simulation

Parameters	Value
k_{P}	7
k_{D}	1
r	0.2 m
I_{w}	0.1 Nm
$I_{i,z}$	0.1 Nm
d	0.9 m
b	0.10 m
m	10 kg
R_{a}	1 ohm
B_{w}	0.1 Nm.sec/rad
k_{a}	10
k_{b}	1

where k_v and k_ω are positive constants. Note that the control law (31) and (32) is not discussed in this paper.

The simulation was designed under a task of reference tracking, i.e., the collision avoidance motion was actually a part of the tracking task. However, in this paper, the reference tracking is not discussed. The proposed collision avoidance motion can be assembled to any moving reference tracking control law.

As shown in Figure 4, the initial configurations of the robots were designed such that there was high possibility to get closer to another robot before reaching their associated references. It could be shown that all the robots were successfully avoided any collision to the others. Figure 5 reveals the performance of reference tracking of each robot. From Figure 5, it can be concluded that the process of target tracking is fully disturbed when the robot's position is in the environment of the obstacle (or, other robots). After the robot exits the environment of the Figure 6 shows that the distances of any pair of robots can exceed the predefined $r_k^{\mathrm{b}} + R_k^{\mathrm{b}}$. For the pairs of robots 1 and 2, 1 and 3, and 2 and 3, we can obtain the closest inter-robot distances were 31.95 meters, 11,76 meters, and 15,19 meters.

5. CONCLUSION

A vector potential function (VPF)-based collision avoidance control algorithm is proposed. The main feature of the control algorithm is that it tracks the linear velocity plan generated by applying VPF in the environment of obstacles. In addition, collision cone principle is considered to examine the safety of the robots. A simulation showing the application of the proposed algorithm on a multiple robot system is presented. It can be proofed that the proposed algorithm.

ACKNOWLEDGEMENT

This work is supported by Laboratorium Pemodelan dan Optimasi, Program Studi Teknik Industri, Universitas Atma Jaya Yogyakarta.

REFERENCES

[1] O. Khatib. "Real-time obstacle avoidance for manipulators and mobile robots," *International Journal of Robotics Research*, vol. 5, no. 1, pp. 90-98, 1986.
[2] E. Rimon and D. E. Koditschek. "Exact robot navigation using artificial potential functions," *IEEE Transactions on Robotics and Automation*, vol. 8, no. 5, pp. 501-518,1992.
[3] M. Erdmann and T. Lozano-Perez. "On multiple objects," *Algorithmica*, vol. 2, pp. 477-521, 1987.
[4] K. J. Kyriakopoulos and G. N. Saridis. "Optimal and suboptimal motion planning for collision avoidance of mobile robots in non-stationary environments," *Journal of Intelligent and Robotics Systems*, vol. 11, pp. 223-267, 1995.
[5] S. S. Ge and Y. J. Cui. "Dynamic motion planning for mobile robots using potential field method," Autonomous Robots, vol. 13, pp. 207-222, 2002.

ISSN: 2252-4274 (Print)
ISSN: 2252-5459 (Online)

[6] A. Widyotriatmo and K.-S. Hong, "Navigation Function-Based Control of Multiple Wheeled Vehicles," *IEEE Transactions on Industrial Electronics*, vol. 58, no. 5, pp. 1896-1906, 2011.
[7] J. Borenstein and Y. Koren. "Real-time obstacle avoidance for fast mobile robots," IEEE Transactions on Systems, Man, and Cybernetics, vol. 19, no. 5, pp. 1179-11897, 1989.
[8] D. Fox, W. Burgard, and S. Thrun. "The dynamic window approach to collision avoidance," *IEEE Robotics & Automation Magazine*, pp. 23-33, March 1997.
[9] J, Minguez and L. Montano. "Nearness diagram (ND) navigation: collision avoidance in troublesome scenarios," *IEEE Transactions on Robotics and Automation*, vol. 20, no.1, pp. 45-59, 2004.
[10] T. Fraichard and H. Asama, "Inevitable collision states – a step towards safer robots?" *Advanced Robotics*, vol. 18, no. 10, 2004, pp. 1001-1024.
[11] A. Cakravarthy and D. Ghose. "Obstacle avoidance in a dynamic environment: a collision cone approach," *IEEE Transactions on Systems, Man, and Cybernetics – Part A: Systems and Humans*, vol. 28, no. 5, pp. 562-574, 1998.
[12] J. Snape, J. van den Berg, S. J. Guy, and D. Manocha. "The hybrid reciprocal velocity obstacle," *IEEE Transactions on Robotics*, vol. 27, no. 4, pp. 696-706, 2011.
[13] K. E. Bekris, D. K. Grady, M. Moll, and L. E. Kavraki, "Safe distributed motion coordination for second-order systems with different planning cycles." *International Journal of Robotics Research*, vol. 31, no. 2, pp. 129-150, 2012.
[14] J. Alonso-Mora, P. Beardsley, and R. Siegwart. "Cooperative collision avoidance for nonholonomic robots," *IEEE Transactions on Robotics*, vol. 34, no. 2, pp. 404-420, 2018.
[15] T. Nguyen, H. M. La, T. D. Le, and M. Jafari, "Formation control and obstacle avoidance of multiple rectangular agents with limited communication ranges," *IEEE Transactions on Control of Network Systems*, vol. 4, no. 4, pp. 680-691, 2017.
[16] D. Zhou, Z. Wang, and M. Schwager. "Agile coordination and assistive collision avoidance for quadrotor swarms using virtual structures," *IEEE Transactions on Robotics*, vol. 34, no. 4, pp. 916-923, 2018.
[17] A. K. Pamosoaji and K.-S. Hong, "A path-planning algorithm using vector potential functions in triangular regions," *IEEE Transactions on Systems, Man, and Cybernetics: Systems*, vol. 43, no. 4, pp. 832-842, 2013.
[18] C. De La Cruz, T. F. Bastos-Filho, and R. Carelli, "Adaptive motion control law of a robotic wheelchair," *Control Engineering Practice*, vol. 19, no. 2, pp. 113-125, 2011.